VOL. 12, NO. 10, MAY 2017 ISSN 1819-6608
ARPN Journal of Engineering and Applied Sciences
©2006-2017 Asian Research Publishing Network (ARPN). All rights reserved.
www.arpnjournals.com

HEMODYNAMIC PREDICTION IN PATENT DUCTUS ARTERIOSUS MORPHOLOGIES

Mohamad Ikhwan Kori[1], Kahar Osman[2] and Ishkrizat Taib[3]
[1]Faculty of Mechanical Engineering, Universiti Teknologi Malaysia, Skudai, Johor Bahru Malaysia
[2]IJN-UTM Cardiovascular Center, Universiti Teknologi Malaysia, Skudai, Johor Bahru, Malaysia
[3]Flow analysis, Simulation and Turbulence Focus Group, Faculty of Mechanical and Manufacturing, Universiti Tun Hussein Onn Malaysia, Parit Raja, Batu Pahat, Johor, Malaysia
E-Mail: kahar@mail.fkm.utm.my

ABSTRACT

Patent ductus arteriosus (PDA) is a condition in which the ductus arteriosus remain opened after birth, causing the blood to shunt through from the aorta to the pulmonary artery. However, due to the complicated nature of the arterial geometry, the flow characteristic inside the PDA is not fully understood, since simplified model are commonly used in researches. This study aims to identify the hemodynamic characteristic in three different patient-specific morphologies. Computational modeling via computational fluid dynamic (CFD) is implemented to predict the blood flow behavior in different PDA morphologies. The result shows that low wall shear stress is observed at the region where the flow recirculation occurs. High wall shear stress is observed in the pulmonary artery due to increase of flow velocity at the insertion point of PDA. The PDA morphologies exhibit left-to-right shunt, which diverts approximately 10% of blood flow from the aorta to the pulmonary artery. The highest shunted blood flow is found in TR LPA morphology. High value of OSI indicates the changes of wall shear stress vector. It is observed that DS LPA has the highest area covered by OSI which presents better hemodynamic characteristic as compared to other morphology.

Keywords: patent ductus arteriosus, computational fluid dynamics, patient-specific geometry.

INTRODUCTION

Ductus arteriosus is a normal fetal blood vessel which connecting the aorta to the pulmonary artery [1]. With PDA, extra blood is pumped from the aorta to the pulmonary arteries. If the PDA was large, the extra blood being pump to the pulmonary arteries makes the heart and lungs work harder and the lungs can become congested. High pressure may occur in the blood vessel, causing damages such as arteriolar medial hyperthrophy, intimal proliferation and fibrosis and eventual obliteration of pulmonary arterioles and capillaries, thus increasing pulmonary resistance [1].

Several types of PDA morphologies were identified by Alwi *et al.* [2]using angiogram images. Due to complicated geometry of the PDA morphology, the characteristic of flow inside the morphology and the effect of various geometry of PDA morphologies to the flow characteristic inside the PDA are not fully understood. Researchers chose to use simplified model of the aorta, PDA and pulmonary arteries geometries in their simulations [3]–[6]. Experimental procedure also being done using devices such as echocardiogram (ECG) and angiogram to determine the hemodynamic effect of the flow to the PDA morphologies. Pekkan *et al* [3] uses idealized model of human fetal aortic arch to visualize the blood flow using in-vitro and computational fluid dynamics (CFD) method. Setchi *et al* [4], [5] in the other hand used mathematical modelling to simulate the flow inside the PDA using simplified PDA morphologies. Taib *et al* [6] also perform CFD simulations on the simplified model of PDA for the stent performance analysis. Thus, using PDA morphology models based on the actual patient PDA aortic arch, pulmonary arteries and PDA geometries are selected to analyze the hemodynamic effect due to different PDA morphologies.

METHODOLOGY

Patient-specific morphology

Three-dimensional PDA morphology surfaces with normal-structured model (left aortic arc) are reconstructed from the computer tomography (CT) images using commercial software called MIMICS (Materialise HQ, Leuven, Belgium). Then, the surface geometries are exported to computer-aided software (CAD) to generate the thickness of the vessel. In this study, three different morphologies are developed and differentiated based on the PDA origin at the aorta and the insertion point to pulmonary artery. The PDA origin can be categorized into ascending aorta (AS), transverse aorta (TR) and descending aorta (DS) while the insertion point is characterized by the main pulmonary artery (MPA), left pulmonary aorta (LPA) and right pulmonary aorta (LPA). The AS has the diameter of 13mm, DS of 6mm, MPA of 11mm, LPA and RPA of 6mm and brachiocephalic, subclavian and carotid arteries with diameters of 3mm. All three morphologies generated are illustrated in Figure-1.

©2006-2017 Asian Research Publishing Network (ARPN). All rights reserved.

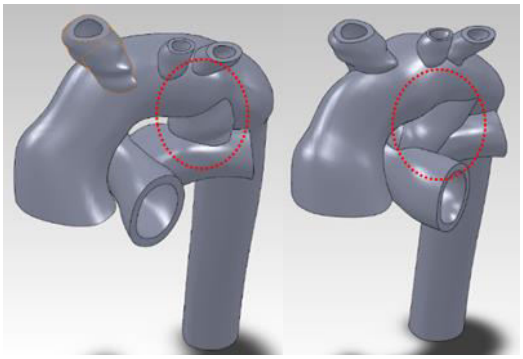

(a) (b)

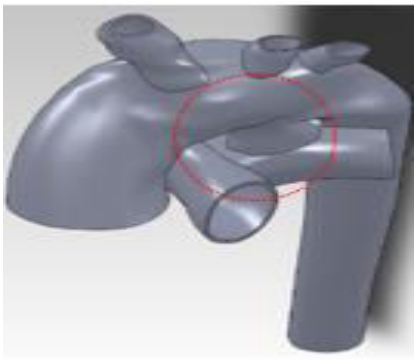

(c)

Figure-1. CAD geometries of PDA morphology.

(a) The PDA origin is at the descending aorta (DS) and the insertion at left pulmonary artery (LPA),
(b) The PDA origin is at the descending aorta (DS) and the insertion at main pulmonary artery (MPA)
(c) The PDA origin is at the transverse aorta (TR) and the insertion at main pulmonary artery (LPA). Red circle indicates the location of PDA.

MATHEMATICAL MODELLING AND SIMULATION

In this study, blood is approximated as Newtonian fluid as the arteries were sufficiently large for this assumption to be valid [7]. The blood density was set at 1060 kg/m^3, with viscosity of 0.00345 N.s/m^2. The vessel wall was assumed to be no slip and rigid wall. The flow is governed by the *Navier-Stokes* equation:

$$\rho\left(\frac{\partial \boldsymbol{u}}{\partial t} + \boldsymbol{u}\cdot\nabla\boldsymbol{u} - f\right) = \mu\nabla^2\boldsymbol{u} - \nabla p \quad (1)$$

$$\nabla\cdot\boldsymbol{u} = 0 \quad (2)$$

Figure-2 illustrates the boundaries assigned to the model. Two inlet boundaries and six outlet boundaries were defined in each model. The inlet boundaries are the aorta inlet and main pulmonary (MPA) inlet. The outlet boundary are the aorta outlet, left pulmonary artery (LPA) outlet, right pulmonary artery (LPA) outlet brachiocephalic artery outlet, carotid artery outlet and the subclavian artery outlet. Pulsatile velocity, shown in Figure-3, was applied at the aorta and MPA inlet based on the result obtained from Pennati *et al* [8]. All the outlet pressure is set to zero for free flow condition. ANSYS CFX software is used to perform the numerical simulation. The solver used finite volume method based on tetrahedral computational mesh in the Cartesian coordinate system.

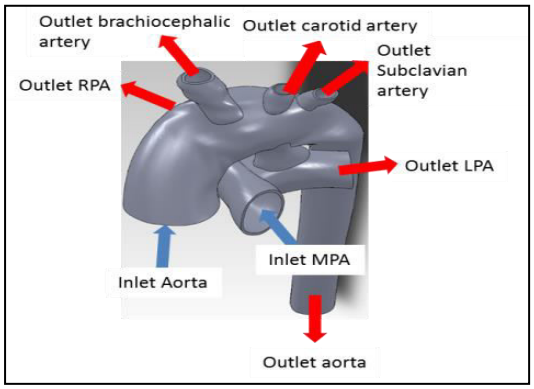

Figure-2. Inlet and outlet boundary conditions of PDA morphologies. Blue arrow indicates inlet boundary while red arrow indicates outlet boundary.

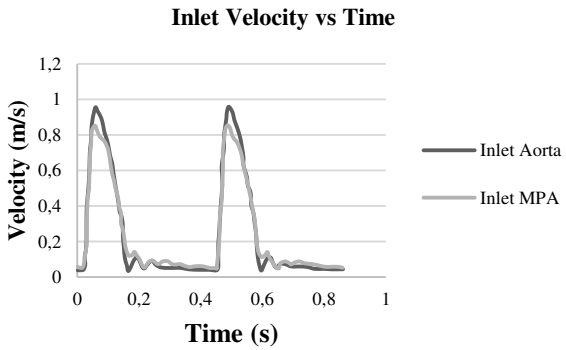

Figure-3. Inlet aorta and MPA velocity vs. time up to 2 cycles.

RESULT AND DISCUSSIONS

Flow characteristic

Helical motion of the blood is observed in all three PDA morphologies, focusing at the ascending aorta before the helical motion recedes as the blood flows to the descending aorta. The helical motion of the blood flow in the aorta is due to the shaped geometry of the aorta especially at the ascending aorta, as observed by Liu *et al* [9]. Due to the helical motion of the flow, the human ascending aorta is insusceptible to the formation of atherosclerotic plaque [9].

The flow inside the aortic branches (brachiocephalic artery, carotid artery and subclavian artery) and PDA for all three morphologies showed that the blood flow focuses at the distal wall of the branches, causing high flow recirculation region. Thus, low velocity profile is observed mainly at the proximal region and high velocity flow at the distal region of the aortic branches. This flow behavior is due to the bifurcating flow coupled with pressure gradient across the branches entry region

©2006-2017 Asian Research Publishing Network (ARPN). All rights reserved.

causing flow stagnation, thus developing secondary flow patterns in the branches [10]. This behavior can be observed by the axial cross section of the branches shown in Figure-5.

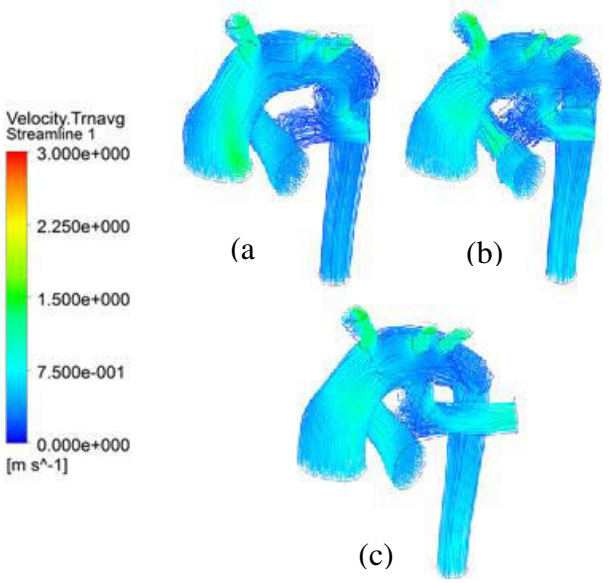

Figure-4. Flow streamline in (a) DS LPA, (b) DS MPA and (c) TR LPA morphologies.

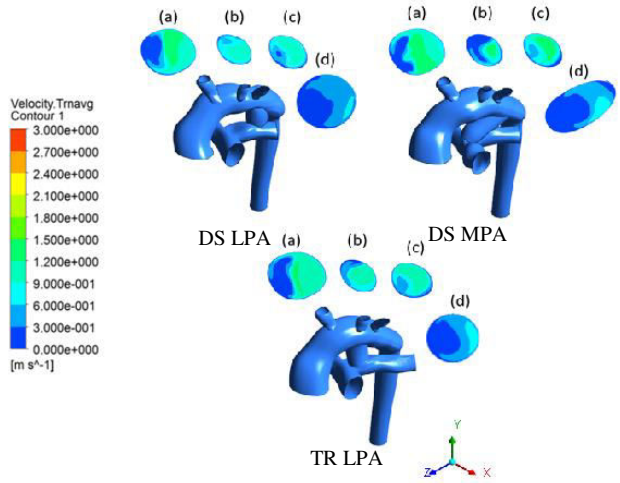

Figure-5. Velocity contour at ZX plane in (a) brachiocephalic artery, (b) carotid artery (c) subclavian artery and (d) PDA.

Velocity increase is observed in the pulmonary artery, especially at the region of the insertion point of the pulmonary artery due to additional flow from the shunted blood flow from the aorta to the pulmonary artery. The velocity contour of the flow near to the insertion area is shown in Figure-5. Blood flow recirculation with low velocity is also observed at the insertion point of the PDA, which is at the proximal of left pulmonary artery for DS LPA and TR LPA morphology while for DS MPA, the flow recirculation is observed at the middle region of main pulmonary artery and proximal of left pulmonary artery.

Maximum flow velocity in PDA is observed during the peak systole stage of the cardiac cycle (0.06s). The highest maximum velocity is observed in DS LPA while the slowest is in DS MPA. The maximum velocities for all morphologies are illustrated in Figure-6. These maximum velocities are still within the range of 0.5 to 2.7 m/s based on the echocardiography measurement performed by Olsson *et al* [11].

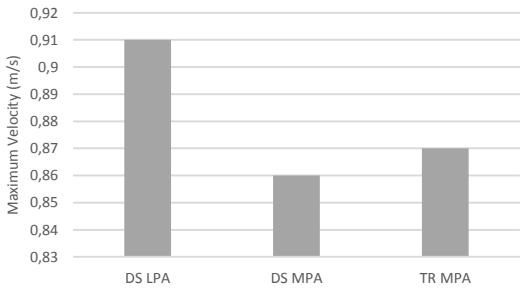

Figure-6. Maximum velocity in PDA at peak systole (0.06s).

Blood distribution

The percentage of average flow rate at the outlet branches of the aorta and pulmonary arteries are determined based on the fraction of flow rate out of the outlet branches from the total flow rate at the inlet of aorta which is 70% from the overall flow in and the main pulmonary artery with the remaining 30%. The percentage of flow rate out from the morphology is illustrated in Figure-7.

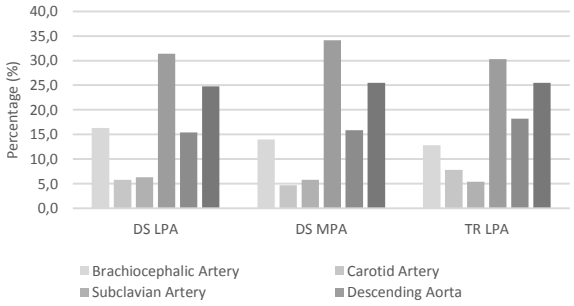

Figure-7. Outflow mass flow rate percentage.

Table-1. Percentage of blood shunted through PDA.

Morphology	DS LPA	DS MPA	TR LPA
% Flow shunted	10.2	11.4	13.7

Analysis of outlet flow rate, as shown in Figure-6, indicates that there is an increase of blood flow shunted from the aorta to the pulmonary artery, or can be described as left-to-right shunt. The percentage of the flow shunted is tabulated in Table-1. Highest flow shunted is in TR LPA and the least in DS LPA morphology. This type of shunt has significant risk to the patient, including pulmonary

©2006-2017 Asian Research Publishing Network (ARPN). All rights reserved.

over circulation and left heart overload [1], causing extra blood to be pumped into the lung arteries, subsequently causing lung congestion. With the oxygenated blood from the systemic circulation is shunted into the pulmonary circulation, cyanosis may be observed especially in the lower extremities of the body. In this case, patient with TR LPA morphology has the highest risk of the said conditions to occur.

Time-averaged wall shear stress (TAWSS)

Low TAWSS is observed at the proximal wall of brachiocephalic artery, carotid artery, subclavian artery and ductus arteriosus. The region of low TAWSS is also observed at the distal of left pulmonary artery, localized at the area of PDA insertion to the pulmonary artery. The region of low TAWSS is observed where the flow recirculation occur, which is low in velocity which promotes platelet activation and plaque buildup [12], as observed in Figure-8. This area of low TAWSS is predicted to be able to induce intima thickening and artherosclerosis development [13], [14].

High TAWSS is observed at the distall wall of the brachiocephalic artery, subclavian artery, carotid artery and ductus arteriosus. High TAWSS is also observed at the distal region of the left pulmonary artery for DS LPA and TR LPA morphologies. For DS MPA morphology, high TAWSS is observed at the middle to the distal region of left pulmonary artery. High TAWSS region in the pulmonary artery is due to the increase of flow caused by the shunt. This region of high TAWSS is predicted to be able to induce endothelial trauma and hemolysis [15].

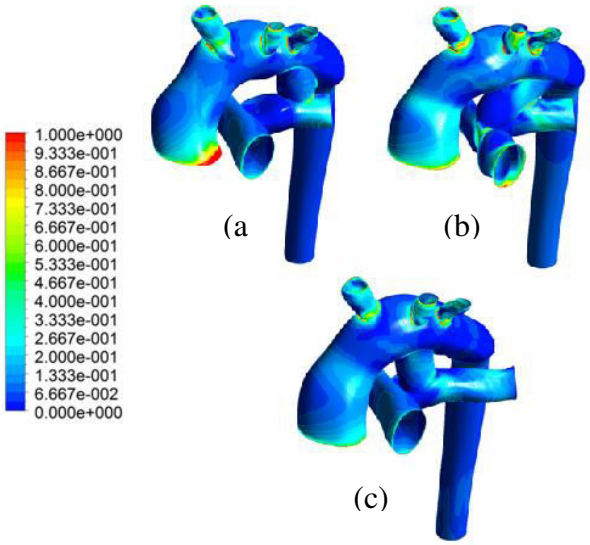

Figure-8. Normalized TAWSS at (a) DS LPA, (b) DS MPA and (c) TR LPA morphology wall.

Oscillatory shear index (OSI)

OSI is proposed to identify the regions where low oscillatory WSS in arteries is occurred [16], in which the OSI value varies from 0 to 0.5. High OSI value with maximum value of 0.5 indicates the area with high deviation of wall shear stress (WSS) direction in cardiac cycle [15]. The regions with high OSI are identified in the outer wall of the ascending aorta, at the PDA wall and the pulmonary artery, especially at the region of PDA insertion at the artery and the distal of the left pulmonary artery. Regions with high value of OSI is prone to atherosclerotic lesion development and may experience an increase of endothelial cell permeability and arterial narrowing [16]. The regions affected by ranges of OSI are illustrated in Figure-9.

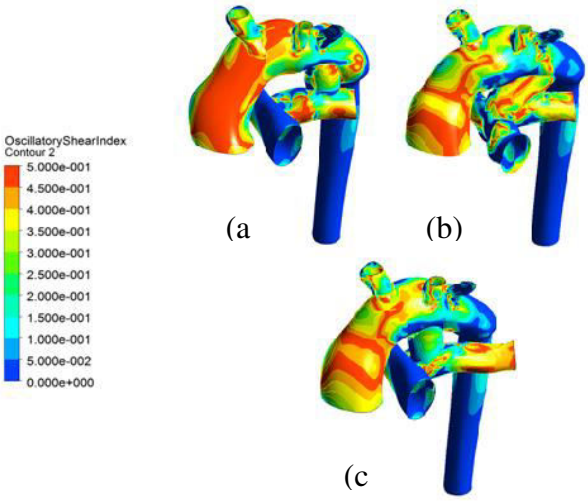

Figure-9. Oscillatory Shear Index at (a) DS LPA, (b) DS MPA and (c) TR LPA morphology wall.

Table-2. Percentage of area covered by OSI.

OSI	Area Covered (%)		
	DS LPA	DS MPA	TR LPA
0 - 0.1	47.23	47.97	46.25
0.1 - 0.2	9.69	10.48	12.69
0.2 - 0.3	11.49	9.46	10.42
0.3 - 0.4	11.43	14.00	12.86
0.4 - 0.5	20.17	18.08	17.77

Glor *et al* [15] stated that the threshold value of OSI is 0.2 before degenerative changes in the arterial wall endothelium occur. Thus, to determine the morphology, which has the highest effect of high OSI to the wall, the percentage area covered is calculated and tabulated in Table-2. DS LPA has the highest area covered with OSI more than 0.2 with 43.08% while the least area is observed in TR LPA with 41.06%, Thus, DS LPA is predicted to be susceptible to the said condition with greater risk as compared to others.

CONCLUSIONS

Low wall shear stress is observed at the region where flow recirculation occurs. High wall shear stress is observed in the pulmonary artery due to increase of flow

©2006-2017 Asian Research Publishing Network (ARPN). All rights reserved.

velocity at the insertion point of PDA. All PDA morphologies exhibit left-to-right shunt, which diverts approximately 10% of blood flow from the aorta to the pulmonary artery. The highest shunted blood flow is found in TR LPA morphology. High value of OSI indicates the changes of wall shear stress vector. DS LPA has the highest area covered by OSI more than 0.2.

ACKNOWLEDGEMENT

The support-of the University of Teknologi Malaysia, under the IJN-UTM Cardiovascular centre grant, lead by Dr. Kahar Osman and under grant number 7845.4F240 is gratefully acknowledged.

REFERENCES

[1] D. J. Schneider and J. W. Moore. 2006. Patent ductus arteriosus. Circulation. 114(17): 1873-82.

[2] M. Alwi. 2012. Stenting the patent ductus arteriosus in duct-dependent pulmonary circulation: techniques, complications and follow-up issues. Future Cardiology. 8(2): 237-250.

[3] K. Pekkan, L. P. Dasi, P. Nourparvar, S. Yerneni, K. Tobita, M. A. Fogel, B. Keller and A. Yoganathan. 2008. In vitro hemodynamic investigation of the embryonic aortic arch at late gestation. Journal of Biomechanics. 41(8): 1697-706.

[4] A. T. Setchi, J. H. Siggers, K. H. Parker, and A. J. Mestel. 2010. Mathematical modeling of two-dimensional flow through patent ductus arteriosus in an adult. 386-389.

[5] A. Setchi, A. J. Mestel, J. H. Siggers, K. H. Parker, M. W. Tan, and K. Wong. 2013. Mathematical model of flow through the patent ductus arteriosus. Journal of Mathematical Biology. 67(6-7): 1487-1506.

[6] I. Taib, M. R. A. Kadir, M. H. S. A. Azis, A. Z. Md Khudzari and K. Osman. 2013. Analysis of hemodynamic differences for stenting patent ductus arteriosus. Journal of Medical Imaging Health Informatics. 3(4): 555-560.

[7] K. Pekkan, O. Dur, K. Sundareswaran, K. Kanter, M. Fogel, A. Yoganathan, and A. Undar. 2008. Neonatal aortic arch hemodynamics and perfusion during cardiopulmonary bypass. Journal of Biomechanics Engineering. 130(6): 061012.

[8] G. Pennati, M. Bellotti, and R. Fumero. 1997. Mathematical modelling of the human foetal cardiovascular system based on Doppler ultrasound data. Medical Engineering and Physics. 19(4): 327-35.

[9] X. Liu, A. Sun, Y. Fan, and X. Deng. 2014. Physiological significance of helical flow in the arterial system and its potential clinical applications. Annals of Biomedical Engineering. 43(1): 3-15.

[10] P. Vasava, P. Jalali, M. Dabagh, and P. J. Kolari. 2012. Finite element modelling of pulsatile blood flow in idealized model of human aortic arch: study of hypotension and hypertension. Computational and Mathematical Methods in Medicine, 2012.

[11] K. W. Olsson, A. Jonzon, and R. Sindelar. 2006. A high ductal flow velocity is associated with successful pharmacological closure of patent ductus arteriosus in infants 22-27 week's gestational age. Critical care research and practice, 2012. 715265.

[12] A. Ceballos. 2011. A multiscale model of the neonatal circulatory system following hybrid norwood palliation (Doctoral dissertation, University of Central Florida Orlando, Florida).

[13] D. Fytanidis, J. Soulis and G. Giannoglou. 2014. Patient-specific arterial system flow oscillation. Hippokratia. 162-165.

[14] A. Gnasso, C. Irace, C. Carallo, M. S. De Franceschi, C. Motti, P. L. Mattioli, and A. Pujia. 1997. In vivo association between low wall shear stress and plaque in subjects with asymmetrical carotid atherosclerosis. Stroke. 28(5): 993-998.

[15] F. P. Glor, B. Ariff, a D. Hughes, L. A. Crowe, P. R. Verdonck, D. C. Barratt, S. A. M. Thom, D. N. Firmin and X. Y. Xu. 2004. Image-based carotid flow reconstruction: a comparison between MRI and ultrasound. Physiology Measurement. 25(6): 1495-1509.

[16] J. Murphy and F. Boyle. 2010. Predicting neointimal hyperplasia in stented arteries using time-dependant computational fluid dynamics: a review. Computers in Biology and Medicine. 40(4): 408-418.